DsbC activation by the N-terminal domain of DsbD

David Goldstone*, Peter W. Haebel*, Federico Katzen†, Martin W. Bader‡, James C. A. Bardwell‡, Jon Beckwith†, and Peter Metcalf*§

*School of Biological Sciences, University of Auckland, Private Bag 92019, Auckland, New Zealand; †Department of Microbiology and Molecular Genetics, Harvard Medical School, Boston, MA 02115; and ‡Department of Biology, University of Michigan, Ann Arbor, MI 48109

Contributed by Jon Beckwith, June 21, 2001

The correct formation of disulfide bonds in the periplasm of *Escherichia coli* involves Dsb proteins, including two related periplasmic disulfide-bond isomerases, DsbC and DsbG. DsbD is a membrane protein required to maintain the functional oxidation state of DsbC and DsbG. In this work, purified proteins were used to investigate the interaction between DsbD and DsbC. A 131-residue N-terminal fragment of DsbD (DsbDα) was expressed and purified and shown to form a functional folded domain. Gel filtration results indicate that DsbDα is monomeric. DsbDα was shown to interact directly with and to reduce the DsbC dimer, thus increasing the isomerase activity of DsbC. The DsbC–DsbDα complex was characterized, and formation of the complex was shown to require the N-terminal dimerization domain of DsbC. These results demonstrate that DsbD interacts directly with full-length DsbC and imply that no other periplasmic components are required to maintain DsbC in the functional reduced state.

The best understood system for the formation of disulfide bonds in folding proteins occurs in the periplasm of Gram-negative bacteria. In *Escherichia coli*, protein disulfide-bond formation depends on the products of *dsb* genes which contain active-site disulfides and are members of the thioredoxin protein superfamily. Five Dsb proteins, DsbA (1, 2), DsbB (3, 4), DsbC (5, 6), DsbD (7), and DsbG (8), have been shown to be involved in disulfide-bond formation and rearrangement. Significant progress has been made in understanding how these proteins interact and function in the periplasm. A search of protein sequence databases revealed that homologs of *E. coli* Dsb proteins occur in many Gram-negative bacteria including early branching thermophiles, suggesting that the system for disulfide-bond formation in the periplasm is widely conserved.

The addition of disulfide bonds within the periplasm is a rapid, nonspecific process (9, 10) catalyzed by the soluble periplasmic protein DsbA (1). DsbA adds disulfide bonds to newly synthesized substrate proteins by donating its active-site disulfide bond (1, 2). Electrons generated by the formation of substrate disulfide bonds are transferred to the DsbA active-site sulfhydryls. The active site of DsbA is regenerated by the transfer of electrons to the integral membrane protein DsbB (4, 11–16) which, in turn, passes electrons to quinone and the electron transport chain (17–20). Incorrect disulfide bonds formed by DsbA may trap proteins in nonnative conformations (10, 21). Disulfide-bond isomerases catalyze the rearrangement of disulfide bonds, allowing proteins trapped by incorrect disulfide bonds to fold correctly. Two homologous enzymes, DsbC and DsbG, facilitate folding of proteins with multiple disulfide bonds in the periplasm (5, 6, 8). Both enzymes are homodimers with protein disulfide-bond isomerase activity (22, 23). The ability of DsbC and DsbG to rearrange incorrect disulfide bonds requires that the active-site cysteines be maintained in the reduced form (24), and both are found almost exclusively in this form in the periplasm (25, 26). The integral membrane protein DsbD transports electrons across the inner membrane of *E. coli* from cytoplasmic thioredoxin (25–30) to the periplasmic target proteins DsbC and DsbG, as well as to the cytochrome *c* biosynthesis pathway via CcmG (also known as DsbE; refs. 28–30). Cells lacking either thioredoxin or DsbD accumulate DsbC and DsbG in the inactive oxidized form (25, 27).

The requirement for the DsbC and DsbG active sites to be reduced raises the question of how this reduction occurs in the oxidizing periplasmic environment. Recent *in vivo* evidence suggests that DsbD does transfer electrons directly to DsbC (30, 31). Apparently, electrons are transferred specifically to the active-site disulfide bonds of oxidized DsbC, DsbG, and CcmG, avoiding the many other disulfide bonds in the periplasm. Little is known about how this specificity is achieved.

The recently determined crystal structure of DsbC revealed a V-shaped homodimer where each DsbC monomer is arranged into two distinct domains (Fig. 1*A*; ref. 32). Residues 78–216, including the CGYC active-site motif (residues 98–101), fold into a domain with a three-dimensional structure similar to that of thioredoxin. The active sites of the thioredoxin domains from each DsbC monomer face inwards across a broad uncharged cleft thought to be the site where folding substrate proteins bind to the molecule. Each of the two thioredoxin domains is connected by a hinged α-helical stalk to a separate central dimerization domain consisting of the N-terminal 65 aa of each 216-residue DsbC monomer (32). Both active sites of the DsbC dimer are required for isomerase activity; the thioredoxin domain alone is inactive (33).

DsbD is arranged into three domains (28, 30): DsbDα, DsbDβ, and DsbDγ (Fig. 1*B*). DsbDα forms a periplasmic domain of 131 residues containing two of the six essential cysteines (C103 and C109) found in DsbD. The central transmembrane domain, DsbDβ (residues 132–429), contains eight predicted transmembrane segments and includes two essential cysteines, C163 in the first transmembrane segment and C285 in the fourth (28, 29). The remaining 135 residues form a second periplasmic domain (DsbDγ) with significant homology to thioredoxin, including a thioredoxin-like active-site motif (CVAC, residues 480–483). Coexpression of all three domains individually restores function to a DsbD-null strain, showing them to function as separate modules (30). Experiments involving the expression of DsbD mutants with systematically mutated cysteines revealed the formation of mixed disulfides between thioredoxin and C163 of DsbDβ and between C98 of DsbC and C109 of DsbDα (30, 31). The latter complex could be observed in cells expressing the mutants DsbC C101A and DsbD C103A (31). These results provide evidence that thioredoxin interacts directly with the central domain of DsbD, and that the N-terminal domain of DsbD interacts directly with DsbC. Katzen and Beckwith (30) have proposed a mechanism in which electrons are accepted from cytoplasmic thioredoxin by DsbDβ. Electrons are thought to pass through the membrane to DsbDγ and then to DsbDα before the reduction of periplasmic targets (30).

Here, we show that the first periplasmic domain of DsbD (DsbDα) is able to form a functional domain, and that it is

Abbreviations: sRNase A, scrambled ribonuclease A; GSSG, glutathione disulfide; AMS, 4-acetamido-4′-maleimidylstilbene-2,2′-disulfonic acid; TCA, trichloroacetic acid.

§To whom reprint requests should be addressed. E-mail: peter.metcalf@auckland.ac.nz.

The publication costs of this article were defrayed in part by page charge payment. This article must therefore be hereby marked "*advertisement*" in accordance with 18 U.S.C. §1734 solely to indicate this fact.

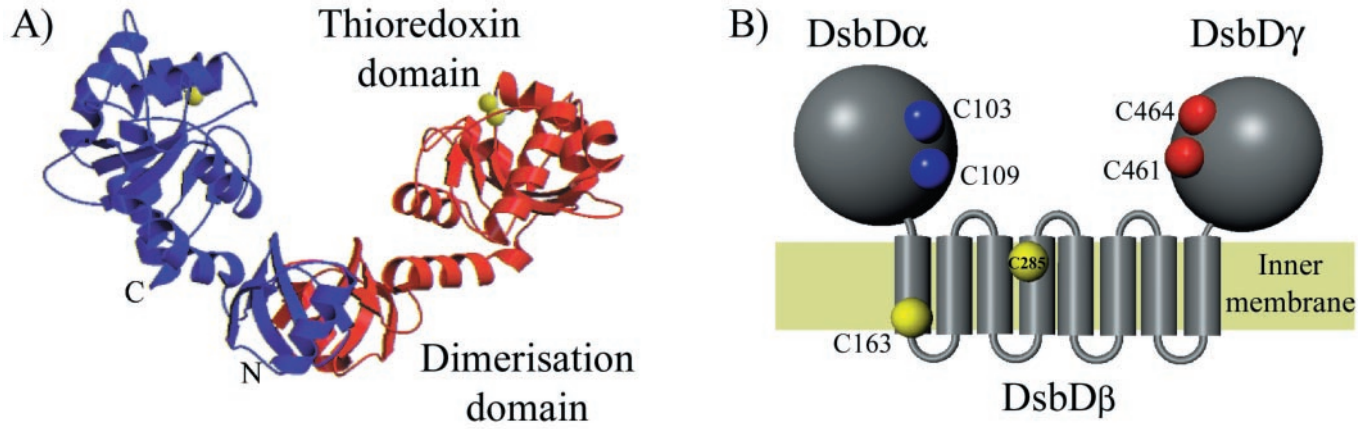

Fig. 1. (*A*) Crystal structure of DsbC: a V-shaped homodimer with each monomer arranged into two distinct domains joined by a short linker helix. The C-terminal thioredoxin domain (residues 78–216) contains the active-site disulfide bond (shown in yellow). The N-terminal dimerization domain (residues 1–65) holds the two monomers together by an extended antiparallel β-sheet. (*B*) The domain structure of DsbD. Each domain contains two essential cysteines. The first 132 residues form a periplasmic domain (DsbDα) followed by eight transmembrane segments (DsbDβ) and a second periplasmic domain thought to be a thioredoxin-like fold (DsbDγ). The first 19 aa are not shown, as these form a cleavable signal sequence that is removed upon insertion into the membrane.

responsible for the final crucial step in activating the periplasmic disulfide-bond isomerase DsbC by reducing its active-site disulfide bond. We prepared the DsbDα–DsbC mixed disulfide complex by using the purified single-cysteine mutants DsbDα C103A and DsbC C101A. Finally, we analyzed the stoichiometry of the complex and showed that complex formation with the thioredoxin domain of DsbC alone does not occur, suggesting that the DsbDα–DsbC interaction requires the complete DsbC molecule.

Methods

Cloning of DsbCC101S-pET22b. DsbC with the active-site mutation C101S was generated by site-directed mutagenesis using the primers pETT7-f (5′-CAC TAT AGG GGA ATT GTG AGC GG-3′), DsbCC121S-f (5′-CC TGT GGT TAC TCC CAC AAA CTG C-3′), DsbCC121S-R (5′-CAG TTT GTG GGA GTA ACC ACA GG-3′), and pETT7-R (5′-CTA GTT ATT GCT CAG CGG TGG CAG C-3′).

DNA coding for the C-terminal thioredoxin-like domain of DsbC lacking the N-terminal dimerization domain (DsbCΔN63 and DsbCΔN63 C101S) was amplified from full-length DsbC and DsbC C101S by using the primers DsbCΔN63-f (5′-GTC AAT GCC ATG GAT AAG ATG CTG-3′) and pETT7-R. The PCR fragment was digested with *Nco*I/*Bam*HI and ligated into linearized pProEX-HTa.

A fragment encoding DsbDα was amplified by PCR from pFK051 (30) by using the primers PQE30 (5′-GAG GGA TCC GAA AAC CTG TAC TTC CAG TCA GGA TTA TTC GAC GCG CCG GGA CGT TCA CAA-3′) and BADREV (5′-ACC GCT TCT GCG TTC TGA TT-3′). The amplified fragment was digested with the enzymes *Bam*HI and *Hin*dIII, and cloned into linearized pQE-30 vector (Qiagen, Chatsworth, CA). The resulting construct pFK115 encodes a cytoplasmic variant of DsbDα peptide in which the signal sequence was replaced by a His_6 tag followed by a tobacco etch virus cleavage site. To generate DsbDα C103A, the codon specifying the first active cysteine of DsbDα was exchanged with that one encoding alanine by using the QuickChange Site-Directed Mutagenesis Kit (Stratagene).

All constructs were verified by DNA sequencing.

Protein Expression and Purification. DsbC was expressed from the plasmid DsbC-pET22b in BL21 (DE3) cells (34), prepared as described (32) by osmotic shock, and purified by anion-exchange chromatography with a Q-Sepharose Fast-Flow column (Amersham Pharmacia) equilibrated with 50 mM Bis-Tris·HCl at pH 6.5. DsbC eluted in a 0–0.4 M NaCl gradient as a single peak, and purity was confirmed by Coomassie blue-stained SDS gels.

DsbC C101S was expressed and purified as described for DsbC, except that DsbC C101S was purified in a NaCl gradient on a Q-Sepharose Fast-Flow anion exchange column equilibrated with 50 mM Tris·HCl at pH 6.8.

DsbDα and DsbDα C103A were expressed in DH5α (Z1) cells (35). Cells were grown overnight to saturation (at 37°C) and induced (at 28°C and 37°C, respectively) with 1 mM isopropyl β-D-thiogalactoside (IPTG). Cells were harvested and lysed by French press; cell lysate was centrifuged at 16,000 × *g* for 30 min to remove cellular debris. Glutathione disulfide (GSSG) was added to a final concentration of 100 μM to ensure that DsbDα was in the oxidized form. Protein was purified by immobilized metal-affinity chromatography on a 5 ml High Trap Chelating column (Amersham Pharmacia) with bound Ni^{2+} equilibrated with 50 mM Hepes, pH 8.0/300 mM NaCl. Both proteins were eluted with 200 mM imidazole. SDS/PAGE showed DsbDα and DsbDα C103A to be essentially pure.

DsbCΔN63 was expressed as described for DsbC and purified by immobilized metal-affinity chromatography as described for DsbDα. DsbCΔN63 was eluted with 250 mM imidazole.

Redox Interactions Between DsbC and DsbDα. DsbC was incubated in 10 mM DTT for 30 min at room temperature to reduce the active-site cysteines. Excess DTT was removed by passage over a PD-10 column (Amersham Pharmacia) equilibrated with 0.1 M sodium phosphate, pH 7.5/1 mM EDTA. DsbDα and DsbDα C103A were reduced as described above by using 50 mM DTT. The number of free cysteines of native and denatured proteins was monitored before and after reduction by using DTNB (Ellman's reagent, 5,5′-dithiobis(2-nitrobenzoic acid; ref. 36). Reduced protein samples were stored at 4°C.

Disulfide exchange between DsbC and DsbDα was investigated by alkylation with 4-acetamido-4′-maleimidylstilbene-2,2′-disulfonic acid (AMS; Molecular Probes). Oxidized and reduced proteins at a final concentration of 10 μM were incubated at 37°C for 90 min in 100 mM sodium phosphate, pH 7.5/1 mM EDTA. Proteins were precipitated and disulfide-exchange reactions were quenched by the addition of trichloroacetic acid (TCA) to a final concentration of 10% for 30 min at 0°C. After centrifugation (16,000 × *g* for 10 min at 4°C), the pellet was

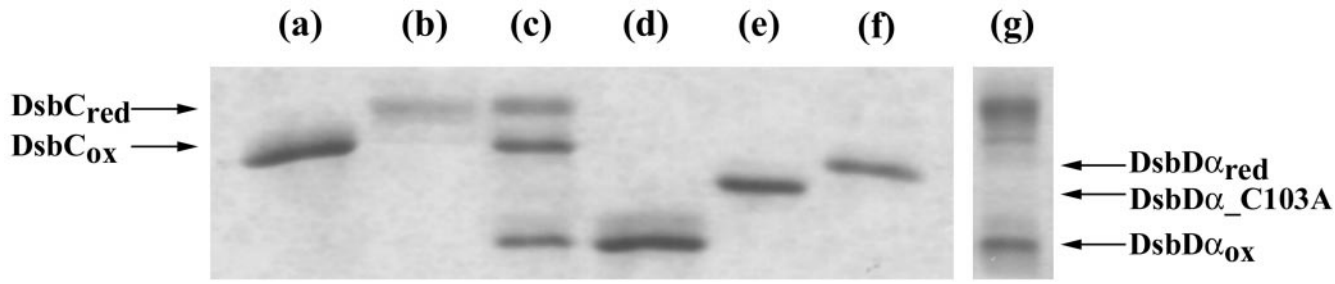

Fig. 2. Disulfide exchange between DsbDα and DsbC. All samples were incubated at 37°C for 90 min before trapping of thiols with 10% (vol/vol) TCA followed by alkylation with AMS. Binding of AMS (≈0.5 kDa) to free thiols caused a visible shift on nonreducing SDS/15% PAGE, which can be used to determine the redox state of each protein within solution. Lane a, oxidized DsbC; lane b, reduced DsbC; lane c, oxidized DsbC + reduced DsbDα; lane d, oxidized DsbDα; lane e, DsbDα C103A; lane f, reduced DsbDα; lane g, oxidized DsbDα + reduced DsbC. Disulfide exchange can be seen to occur between reduced DsbDα and oxidized DsbC. No exchange occurs in the reverse reaction between reduced DsbC and oxidized DsbDα. The relative position of each species is indicated.

resuspended in 1 M Tris·HCl, pH 8.0/1 mM EDTA/1% SDS/10 mM AMS (Molecular Probes) and incubated for 90 min at 37°C. Proteins were reprecipitated with 1 ml of ice-cold acetone and pelleted. The pellet was resuspended in nonreducing Laemmli buffer and heated for 5 min at 96°C before separation by SDS/15% PAGE.

Disulfide-Bond Isomerase Assay. *Preparation of scrambled RNase A (sRNase A).* RNase A (10 mg; Sigma) was denatured and reduced in 1 ml of 0.1 M Tris·HCl, pH 8.0/2 mM EDTA/6 M guanidinium·HCl/140 mM DTT at 37°C for 1 hr. Buffer was exchanged to 0.1% acetic acid over a PD-10 column. Denatured and reduced RNase A (10 μM) was oxidized in 0.1 μM DsbA/0.1 μM DsbB/50 μM 2,3-dimethoxy-5-methyl-6-decyl-1,4-benzoquinone (quinone, Q_0C_{10}) in 0.1 M sodium phosphate buffer (pH 6.0) and 0.1% *n*-dodecyl β-D-maltoside (Sigma). sRNase A was purified by gel filtration on a Superdex 75 16/60 column (Amersham Pharmacia) equilibrated with 0.1 M Tris·HCl (pH 8.0). Individual fractions were stored at 4°C.

Isomerase assay. Protein Samples of 2 μM were incubated with 5 μM sRNase A in 0.1 M sodium phosphate buffer, pH 7.5/1 mM EDTA adjusted to a final volume of 1 ml. After 2 hr at room temperature, 4.5 mM cytidine 2′,3′-cyclic monophosphate (cCMP) was added, and RNase A activity was determined by measuring absorbance at 296 nm over 20 min.

Complex Formation Between DsbDα C103A and DsbC. DsbC and DsbDα proteins were mixed at ratios of 1:2 (0.2 mM + 0.4 mM) in the absence of any redox reagent or in the presence of either 20 mM GSSG as oxidant or 20 mM DTT as reductant. The protein mixtures were incubated at room temperature for at least 1 hr. Samples of 100 μl each were analyzed by gel filtration followed by peak analysis on reducing and nonreducing SDS/PAGE.

Complex formation between DsbDα and DsbC was determined by molecular-weight analysis. Gel filtration chromatography was used to estimate the molecular masses of native and mutant proteins and complexes. All experiments were carried out in 50 mM Tris·HCl, pH 8.0/200 mM NaCl by using a Superdex 75 HR0/30 gel filtration column (Amersham Pharmacia) on an ÄKTA Explorer FPLC System (Amersham Pharmacia) at a flow rate of 1.5 ml/min.

The column was calibrated with the low molecular weight gel filtration calibration kit from Amersham Pharmacia.

Determination of Protein Concentration. All protein concentrations were determined by UV absorption at 280 nm by using the following calculated (37) extinction coefficients: DsbDα C103A, 21,620 $M^{-1}\cdot cm^{-1}$; DsbDα, 21,740 $M^{-1}\cdot cm^{-1}$; DsbC, 16,170 $M^{-1}\cdot cm^{-1}$; DsbC C101S, 16,050 $M^{-1}\cdot cm^{-1}$; DsbCΔN63, 13,610 $M^{-1}\cdot cm^{-1}$; and DsbC C101SΔN63, 13,490 $M^{-1}\cdot cm^{-1}$. All concentrations were calculated for monomeric protein.

Results

DsbDα Forms a Soluble Monomeric Domain with Both Cysteines Exposed. To obtain the isolated α-domain of DsbD, a construct (DsbDα) containing residues 1–131 of DsbD and preceded by an N-terminal His_6 tag and a nine-residue flexible linker segment containing a tobacco etch virus (TEV) protease cleavage site was expressed and purified from total cell lysate under oxidizing conditions (100 μM GSSG) by immobilized metal-affinity chromatography. Subsequent experiments demonstrated that the protein was active without removal of the N-terminal extension; therefore, the TEV protease cleavage site was not used (data not shown). The purified DsbDα protein could be concentrated to at least 20 mg/ml without aggregation. The apparent molecular mass estimated from SDS/PAGE was ≈18 kDa, consistent with the calculated value from the DNA sequence (17.1 kDa). The molecular mass of native DsbDα was estimated by comparison with known standards by using gel filtration chromatography. Both DsbDα and DsbDα C103A eluted with an apparent molecular mass of 25 kDa (K_{av} = 0.25), confirming that they are monomeric in solution and suggesting a somewhat extended conformation (increased apparent molecular masses are expected for nonspherical molecules).

DsbDα and DsbDα C103A were reduced by using 50 mM DTT and the resultant free thiol molar ratio was estimated by using DTNB (Ellman's reagent). Both cysteine residues of DsbDα were accessible (1.6 thiol per mol) as was C109 of the single-cysteine mutant DsbDα C103A (0.6 thiols per mol). The redox status of DsbDα was also investigated by using AMS, an ≈500-Da reagent that covalently labels free thiols. Proteins were fixed and denatured with 10% (vol/vol) TCA before AMS labeling and analyzed under nonreducing conditions with SDS/PAGE. The bound AMS caused a visible shift in mobility. Reduced and oxidized DsbDα, as also DsbDα C103A, migrate as single bands, and AMS band-shifts were observed that clearly distinguished all three molecules (Fig. 2).

DsbDα Reduces DsbC. When reduced DsbDα and oxidized DsbC were mixed, both proteins showed redox changes consistent with quantitative disulfide-bond transfer from DsbC to DsbDα (Fig. 2, lane c). Equal amounts of oxidized DsbDα and reduced DsbC were observed as expected for the transfer of electrons from one DsbDα molecule to one DsbC monomer. The presence of some remaining oxidized DsbC suggests that the reaction had proceeded to completion and that no remaining reduced DsbDα was present to reduce DsbC. No shift in redox state was observed in the reverse reaction when reduced DsbC was mixed with oxidized DsbDα (Fig. 2, lane g). No evidence of the mixed disulfide

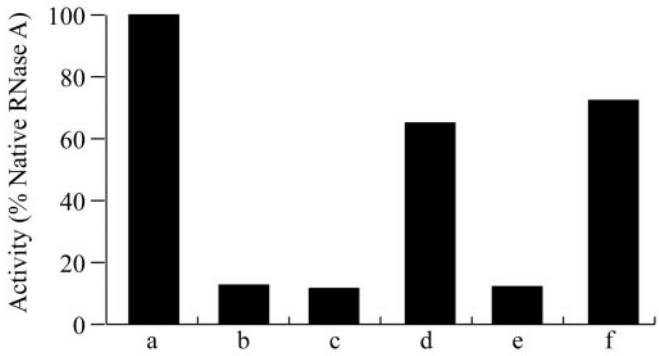

Fig. 3. Reduced DsbDα is able to activate oxidized DsbC. Protein samples of 2 μM, including a mix of 2 μM oxidized DsbC and 2 μM reduced DsbDα, were incubated with 5 μM sRNase A at room temperature for 2 hr. cCMP was added to 4.5 μM final concentration. RNase A activity was determined by measuring the change in absorbance at 296 nm caused by the cleavage of the cCMP by active RNase A. The relative activity of each sample compared with native RNase A is shown. Bar a, 5 μM native RNase A; bar b, 5 μM sRNase A alone; bar c, sRNase A + oxidized DsbC; bar d, sRNase A + reduced DsbDα + oxidized DsbC; bar e, sRNase A + reduced DsbDα; and bar f, reduced DsbC. Samples were measured in triplicate. A typical result is shown.

complex between DsbC and DsbDα was observed after trapping with TCA.

DsbDα Activates DsbC. The disulfide-bond isomerase activity of DsbC was assessed to determine whether DsbC is activated after reduction by DsbDα. Disulfide-bond isomerase activity was assayed by measuring the recovery of misfolded sRNase A (38). The refolding of denatured and reduced RNase A by using the DsbA/DsbB oxidizing pathway rapidly adds stable disulfide bonds linking randomly paired cysteines. This addition causes much of the protein to become trapped in inactive (i.e., scrambled) conformations (10). sRNase A, consisting almost entirely of inactive RNase A, can then be purified from the refolding mixture. Reduced DsbC is able to resolve the incorrect disulfide bonds in sRNase A, thus restoring activity (16, 39).

The sRNase A alone showed an activity of only 12% that of native RNase A (Fig. 3). The addition of oxidized DsbC or reduced DsbDα separately made no appreciable difference to this background level of activity. The mixture of 2 μM reduced DsbDα with 2 μM oxidized DsbC, however, activated the sRNase A to levels similar to that achieved with 2 μM chemically reduced DsbC (72% native RNase A activity), demonstrating that reduction by DsbDα activates DsbC.

Complex Formation Between DsbDα and DsbC. Having shown that DsbDα activates DsbC, we investigated the interaction between these two proteins by examining the formation of mixed disulfide intermediates. Removal of the first cysteine of DsbDα (C103) traps the disulfide-exchange reaction as a mixed disulfide intermediate (30, 31). A similar stable complex was observed when DsbDα C103A was mixed with DsbC modified to remove the second active-site cysteine (C101) which might otherwise resolve the mixed-disulfide complex. In these experiments, a 2-fold excess of DsbDα was added to DsbC that was incubated under reducing and oxidizing conditions; the products were purified by gel filtration chromatography (Fig. 4) and analyzed by both reducing and nonreducing SDS/PAGE (Fig. 5).

Both DsbC and DsbC C101S eluted with an apparent molecular mass of 63 kDa ($K_{av} = 0.10$) in accordance with the extended conformation of the 46-kDa DsbC dimer. DsbDα C103A forms complexes with both DsbC C101S (Fig. 4*A*) and oxidized DsbC (Fig. 4*B*), as indicated by a shift of the DsbC peak to the higher

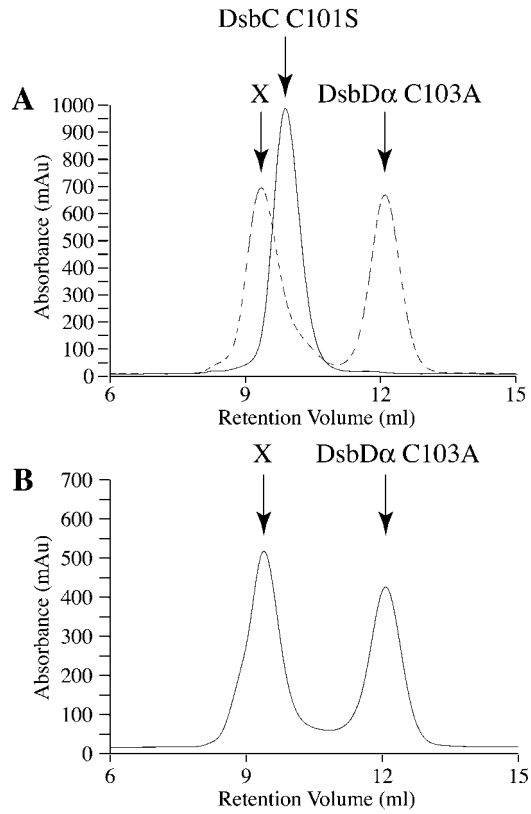

Fig. 4. Size-exclusion chromatography of DsbDα C103A–DsbC C101S complex. Samples were mixed and incubated before separation by size-exclusion chromatography. (*A*) Elution profiles for DsbC C101S (solid line) and DsbC C101S + DsbDα C103A mix (dashed line) are shown. mAu, 0.001 absorbance unit at 280 nm. Peak fractions were analyzed by SDS/PAGE. DsbC C101S was eluted with an apparent molecular mass of 63 kDa ($K_{av} = 0.10$). The addition of excess DsbDα resulted in a shift to an apparent molecular mass of 70 kDa (X, $K_{av} = 0.08$). (*B*) A similar elution profile was seen when native oxidized DsbC was mixed with excess DsbDα C103A. The peak at X corresponds to the DsbC–DsbDα C103A complex. No complex formation was observed when the proteins were mixed in the presence of 20 mM DTT (data not shown).

apparent molecular mass of 70 kDa ($K_{av} = 0.08$) when DsbDα C103A was added under nonreducing conditions. These complexes could be dissociated by the addition of 20 mM DTT, suggesting that they are held together by a disulfide bond (data not shown).

The purified DsbC C101S-DsbDα C103A complex showed two bands on reducing SDS/PAGE (Fig. 5, lanes 4 and 5). The 26-kDa band corresponds to DsbC C101S, and the 18-kDa band corresponds to DsbDα C103A. The ratio of the band intensities is $\approx$2:1. Nonreducing SDS/PAGE also revealed two bands (Fig. 5, lanes 8 and 9). The lower of these bands (26 kDa) corresponds to DsbC C101S; the higher molecular mass DTT-sensitive band matches the expected molecular mass of the DsbC C101S–DsbDα C103A disulfide-linked complex (44 kDa = 26 kDa + 18 kDa). Denaturation of the disulfide-linked complex under nonreducing conditions produces both molecules composing DsbC monomers disulfide-linked to DsbDα and also uncomplexed DsbC monomers in approximately equal amounts.

We estimate the stoichiometry of the DsbC–DsbDα complex to be 2:1, based on the sizing column apparent molecular mass (70 kDa) and the results of the reducing and nonreducing gels. This estimate corresponds to a complex of a dimeric DsbC molecule bound to a single DsbDα molecule. Similar results were obtained when DsbC C101S was incubated with increasing amounts of DsbDα C103A (data not shown). No evidence was

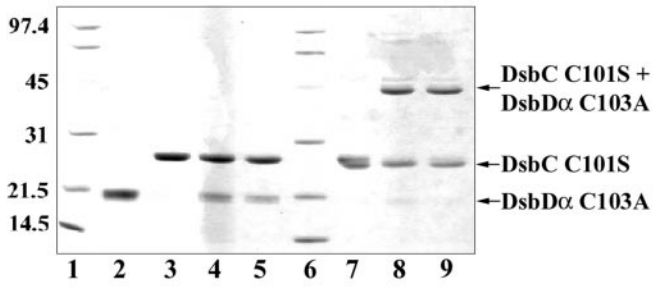

Fig. 5. Analysis of DsbC C101S–DsbDα C103A complex formation. DsbC C101S and DsbDα C103A were mixed in the presence or absence of either 20 mM DTT or 20 mM GSSG and separated by size-exclusion chromatography (Fig. 4*A*). The first eluted peak in each experiment was analyzed by both reducing (lanes 3–5) and nonreducing (lanes 7–9) SDS/PAGE. A DTT-sensitive band in peak fractions (Fig. 4*A*, peak X) corresponding to the disulfide-linked complex between DsbC C101S and DsbDα C103A is evident by nonreducing SDS/PAGE (upper band in lanes 8 and 9). Free DsbC C101S is also visible after complex formation (lower band in lanes 8 and 9). The disulfide-linked complex is not visible after separation by reducing SDS/PAGE (lanes 4 and 5). The ratio of DsbC C101S to DsbDα C103A in the complex peak, which was purified by size-exclusion chromatography and analyzed by reducing SDS/PAGE, is $\approx$2:1 (lanes 4 and 5). Complex formation is evident in the presence (lanes 5 and 9) or absence (lanes 4 and 8) of 20 mM GSSG. No complex formation is observed when the proteins are mixed in the presence of 20 mM DTT (lanes 3 and 7; the first eluted peak is DsbC C101S). Molecular mass markers are shown in lanes 1 and 6. Lane 2 is DsbDα C103A. Markers and DsbDα C103A were run under reducing conditions.

observed for a complex consisting of a DsbC dimer bound to two DsbDα molecules. No complex formation was observed between DsbC C101S and oxidized DsbDα, showing that complex formation does depend on protein redox states (data not shown).

The N-terminal Dimerization Domain of DsbC Is Required for Complex Formation. No complex formation was observed between DsbDα C103A and the thioredoxin domain of DsbC (DsbCΔN63 and DsbCΔN63 C101S) with or without 20 mM GSSG (data not shown). Although an intermolecular disulfide bond joins DsbDα to the active site of full-length DsbC, no binding to the same active site of the DsbC thioredoxin domain alone was observed. The lack of binding to the isolated DsbC thioredoxin domain, even under oxidizing conditions, suggests that the DsbC N-terminal domain is essential for the interaction between these two proteins.

Discussion

Periplasmic disulfide-bond formation requires both highly specific and nonspecific protein interactions mediated by mixed disulfide-bond intermediates. The electron-transport interaction between DsbC and its reductant DsbD occurs in an oxidizing environment and is likely to be highly specific and insulated from the numerous disulfide bonds in the periplasm. DsbD should be able to distinguish between the active-site disulfide bonds of substrates such as DsbC and DsbG and other disulfides within the periplasm. By contrast, the substrate-binding interactions of DsbC are sufficiently nonspecific to allow the successful periplasmic expression of recombinant nonbacterial proteins containing multiple disulfide bonds (40–44). We are interested in learning how DsbC participates in these very different types of interaction.

In this work, we have used purified proteins together with disulfide-bond formation and isomerase assays to investigate the interaction between DsbC and DsbD. First, we expressed and purified DsbDα and then used gel filtration and DTT reduction to show that both DsbDα and DsbDα C103A are monomers with solvent-accessible cysteines. The stability and solubility of DsbDα and DsbDα C103A indicate that these domains are folded.

The results of experiments involving sulfhydryl labeling of mixtures of purified DsbC and DsbDα in defined redox states together with protein disulfide-bond isomerase assays showed that DsbDα can reduce and fully activate oxidized DsbC. These results are consistent with those of Katzen and Beckwith (30), who presented *in vivo* evidence that DsbDα interacts directly with DsbC. The results also demonstrate that no other periplasmic components are required to maintain DsbC in the functional reduced state. There was no evidence for the reverse reaction, and no disulfide-bond transfer was observed in mixtures of oxidized DsbDα and reduced native DsbC. Complex formation could be seen by using the cysteine mutant DsbDα C103A, as observed earlier *in vivo* (30). The absence of an observable mixed disulfide intermediate between DsbDα and native DsbC after trapping with TCA suggests that the exchange of disulfide bonds from DsbC to DsbDα is rapid. Complex formation was observed with both native DsbC and DsbC C101S, the latter presumably a result of oxidation by air. Analysis by gel filtration of the mixed disulfide complex formed between DsbDα C103A and DsbC C101S showed that a single DsbDα molecule bound a DsbC dimer. No complex formation was observed when the thioredoxin domain of DsbC alone was substituted for full-length DsbC in these experiments. This result implies that regions of DsbC distant from the active site are required for complex formation to occur. For this reason, it is unlikely that the reaction is simply a consequence of the comparative active-site redox potentials of DsbC and DsbDα.

Many questions remain about the interaction of DsbD and DsbC. We envisage the interaction surface between the DsbDα monomer and the DsbC dimer as including the disulfide bond at either one of the two DsbC active sites and extending beyond the DsbC thioredoxin domain, possibly to include parts of both thioredoxin domains. Docking of the two molecules is followed by the formation of a mixed disulfide bond between one of the two DsbC active-site C98 residues and C109 from the DsbDα monomer. After transfer of electrons from DsbD and formation of the DsbD C109-C103 disulfide bond, conformational changes occur in one or both partners, causing the complex to disassemble.

What determines the specificity of the DsbDα–DsbC interaction? How is the reduced DsbD active site protected from other disulfide bonds in the periplasm? The answers to these questions will clearly require detailed information on binding kinetics together with more three-dimensional structures. The observation that single-cysteine mutants of DsbDα are prone to degradation within the cell (30) leads us to speculate that the reduced DsbDα active site may be locally unfolded. We hypothesize that this locally unfolded conformation mimics the binding of unfolded substrate proteins to DsbC, which is thought to occur at the large, uncharged cleft between the two active sites (32, 39). Electron transfer and the subsequent formation of the DsbDα active-site disulfide bond would then cause a local transition to a more folded, less hydrophobic structure and release DsbDα from the DsbC binding cleft. According to this hypothesis, reduced DsbDα would be protected from disulfide bonds in nonhydrophobic environments such as those in folded proteins. Specificity of the DsbC–DsbDα interaction could be accounted for by the ability of DsbC to bind unfolded substrates, and more importantly, by the redox-coupled local conformational change in DsbDα, allowing only the reduced molecule to bind to DsbC. Further protein crystallographic structural investigations of DsbDα, DsbDα C103A, and the DsbC–DsbDα complex may shed light on the proposed DsbDα active-site structural transition.

P.W.H. is supported by Boehringer Ingelheim Fonds, and F.K. is sponsored by the Pew Charitable Trusts. This study was supported by a National Institutes of Health grant to J.C.A.B. The J.B. laboratory work was supported by Grant GM55090 from the National Institutes of Health, and the P.M. laboratory work was supported by the New Zealand Health Research Council. J.C.A.B. is a Pew scholar, F.K. is a Pew Latin American fellow in the Biomedical Sciences, and J.B. is an American Cancer Society Research Professor.

1. Bardwell, J. C., McGovern, K. & Beckwith, J. (1991) *Cell* **67,** 581–589.
2. Akiyama, Y., Kamitani, S., Kusukawa, N. & Ito, K. (1992) *J. Biol. Chem.* **267,** 22440–22445.
3. Missiakas, D., Georgopoulos, C. & Raina, S. (1993) *Proc. Natl. Acad. Sci. USA* **90,** 7084–7088.
4. Bardwell, J. C., Lee, J. O., Jander, G., Martin, N., Belin, D. & Beckwith, J. (1993) *Proc. Natl. Acad. Sci. USA* **90,** 1038–1042.
5. Shevchik, V. E., Condemine, G. & Robert-Baudouy, J. (1994) *EMBO J.* **13,** 2007–2012.
6. Missiakas, D., Georgopoulos, C. & Raina, S. (1994) *EMBO J.* **13,** 2013–2020.
7. Missiakas, D., Schwager, F. & Raina, S. (1995) *EMBO J.* **14,** 3415–3424.
8. Andersen, C. L., Matthey-Dupraz, A., Missiakas, D. & Raina, S. (1997) *Mol. Microbiol.* **26,** 121–132.
9. Zapun, A., Bardwell, J. C. & Creighton, T. E. (1993) *Biochemistry* **32,** 5083–5092.
10. Bader, M. W., Xie, T., Yu, C. A. & Bardwell, J. C. (2000) *J. Biol. Chem.* **275,** 26082–26088.
11. Dailey, F. E. & Berg, H. C. (1993) *Proc. Natl. Acad. Sci. USA* **90,** 1043–1047.
12. Jander, G., Martin, N. L. & Beckwith, J. (1994) *EMBO J.* **13,** 5121–5127.
13. Guilhot, C., Jander, G., Martin, N. L. & Beckwith, J. (1995) *Proc. Natl. Acad. Sci. USA* **92,** 9895–9899.
14. Kishigami, S., Kanaya, E., Kikuchi, M. & Ito, K. (1995) *J. Biol. Chem.* **270,** 17072–17074.
15. Kishigami, S., Akiyama, Y. & Ito, K. (1995) *FEBS Lett.* **364,** 55–58.
16. Bader, M., Muse, W., Zander, T. & Bardwell, J. (1998) *J. Biol. Chem.* **273,** 10302–10307.
17. Bader, M., Muse, W., Ballou, D. P., Gassner, C. & Bardwell, J. C. (1999) *Cell* **98,** 217–227.
18. Kobayashi, T., Kishigami, S., Sone, M., Inokuchi, H., Mogi, T. & Ito, K. (1997) *Proc. Natl. Acad. Sci. USA* **94,** 11857–11862.
19. Zeng, H., Snavely, I., Zamorano, P. & Javor, G. T. (1998) *J. Bacteriol.* **180,** 3681–3685.
20. Kobayashi, T. & Ito, K. (1999) *EMBO J.* **18,** 1192–1198.
21. Gilbert, H. F. (1997) *J. Biol. Chem.* **272,** 29399–29402.
22. Zapun, A., Missiakas, D., Raina, S. & Creighton, T. E. (1995) *Biochemistry* **34,** 5075–5089.
23. Bessette, P. H., Cotto, J. J., Gilbert, H. F. & Georgiou, G. (1999) *J. Biol. Chem.* **274,** 7784–7792.
24. Darby, N. J., Raina, S. & Creighton, T. E. (1998) *Biochemistry* **37,** 783–791.
25. Joly, J. C. & Swartz, J. R. (1997) *Biochemistry* **36,** 10067–10072.
26. Rietsch, A., Belin, D., Martin, N. & Beckwith, J. (1996) *Proc. Natl. Acad. Sci. USA* **93,** 13048–13053.
27. Rietsch, A., Bessette, P., Georgiou, G. & Beckwith, J. (1997) *J. Bacteriol.* **179,** 6602–6608.
28. Stewart, E. J., Katzen, F. & Beckwith, J. (1999) *EMBO J.* **18,** 5963–5971.
29. Chung, J., Chen, T. & Missiakas, D. (2000) *Mol. Microbiol.* **35,** 1099–1109.
30. Katzen, F. & Beckwith, J. (2000) *Cell* **103,** 769–779.
31. Krupp, R., Chan, C. & Missiakas, D. (2001) *J. Biol. Chem.* **276,** 3696–3701.
32. McCarthy, A. A., Haebel, P. W., Torronen, A., Rybin, V., Baker, E. N. & Metcalf, P. (2000) *Nat. Struct. Biol.* **7,** 196–199.
33. Sun, X. X. & Wang, C. C. (2000) *J. Biol. Chem.* **275,** 22743–22749.
34. Studier, F. W., Rosenberg, A. H., Dunn, J. J. & Dubendorff, J. W. (1990) *Methods Enzymol.* **185,** 60–89.
35. Lutz, R. & Bujard, H. (1997) *Nucleic Acids Res.* **25,** 1203–1210.
36. Riddles, P. W., Blakeley, R. L. & Zerner, B. (1983) *Methods Enzymol.* **91,** 49–60.
37. Gill, S. C. & von Hippel, P. H. (1989) *Anal. Biochem.* **182,** 319–326.
38. Lundstrom-Ljung, J. & Holmgren, A. (1995) *J. Biol. Chem.* **270,** 7822–7828.
39. Chen, J., Song, J. L., Zhang, S., Wang, Y., Cui, D. F. & Wang, C. C. (1999) *J. Biol. Chem.* **274,** 19601–19605.
40. Bessette, P. H., Aslund, F., Beckwith, J. & Georgiou, G. (1999) *Proc. Natl. Acad. Sci. USA* **96,** 13703–13708.
41. Kurokawa, Y., Yanagi, H. & Yura, T. (2000) *Appl. Environ. Microbiol.* **66,** 3960–3965.
42. Joly, J. C., Leung, W. S. & Swartz, J. R. (1998) *Proc. Natl. Acad. Sci. USA* **95,** 2773–2777.
43. Schmidt, A. M., Bloss, I. & Skerra, A. (1998) *Protein Eng.* **11,** 601–607.
44. Qiu, J., Swartz, J. R. & Georgiou, G. (1998) *Appl. Environ. Microbiol.* **64,** 4891–4896.